





Impact of Accelerated Carbonation on Microstructure and Phase Assemblage

	<p>Andres Belda Revert PhD student Norwegian University of Science and Technology (NTNU), Department of Structural Engineering Richard Birkelands vei 1 A, 7491. Trondheim andres.b.revert@ntnu.no</p>
	<p>Klaartje De Weerd PhD, Associate Professor Norwegian University of Science and Technology (NTNU), Department of Structural Engineering Richard Birkelands vei 1 A, 7491. Trondheim klaartje.d.weerd@ntnu.no</p>
	<p>Ulla Hjorth Jakobsen PhD, Senior Consultant Danish Technological Institute (DTI) Concrete Centre Gregersensvej 4, DK 2630 Taastrup uhj@teknologisk.dk</p>
	<p>Mette Rica Geiker PhD, Professor Norwegian University of Science and Technology (NTNU), Department of Structural Engineering Richard Birkelands vei 1 A, 7491. Trondheim mette.geiker@ntnu.no</p>

ABSTRACT

The paper summarizes preliminary results on characterization of the microstructure and phase assemblage of mortar and concrete samples containing Portland and Portland-fly ash cement carbonated at either natural conditions, 60% *RH* and 1% CO_2 , 90% *RH* and 5% CO_2 or 60% *RH* and 100% CO_2 . Different characterization techniques were used: thermogravimetric analysis to study the solid phases, SEM-EDS point analysis to investigate the chemical composition of the solid phases, optical microscopy to investigate the microstructure, and cold water extraction to characterize the chemical composition of the pore solution. The combined results on microstructure and phase assemblage indicate that carbonation up to 5% CO_2 appears representative for natural carbonation. Pore solution analysis revealed similar trends for the three accelerated carbonation conditions.

Key words: Carbonation, microstructure, solid phases, pore solution, Portland-fly ash cement

1. INTRODUCTION

Carbonation is the reaction of the CO₂ present in the atmosphere with the phases in the hydrated cement paste. Carbonation causes a change in the microstructure, solid phases, and lowers the pH of the pore solution [1]. Carbonation in natural exposure is a slow process. For performance testing, carbonation is therefore usually accelerated by means of optimal relative humidity (60-70%) [1] and increased CO₂ concentration (25-250 times higher than natural) [2]. However, it is not clear to which extent the microstructure and phase assemblage developed upon accelerated carbonation mirrors that for natural carbonation.

Castellote et al. [3] investigated cement paste exposed to various CO₂ concentrations (0.03 (natural), 3, 10 and 100%). The samples were prepared with Portland cement and a water-to-binder ratio (*w/b*) of 0.5. Phase changes due to carbonation were investigated using ²⁹Si solid-state nuclear magnetic resonance (²⁹Si MAS-NMR), thermogravimetry (TGA) and x-ray diffraction (XRD). The authors concluded that accelerated carbonation up to 3% CO₂ gives similar products compared to natural carbonation. For 10% and 100% CO₂ the C-S-H was more extensively carbonated and silica gel was formed.

Auroy et al. [4] investigated cement paste (*w/b* = 0.40) containing a ternary blend (50% PC + 25% FA + 25% GGBFS). Exposure conditions were 25°C, 55% RH, and 0.04 or 3% CO₂. Carbonation was investigated using XRD, TGA and ²⁹Si NMR. They found that similar products were formed upon carbonation at the two different CO₂ concentrations. Some calcium hydroxide was found in the carbonated area, and C-S-H decomposed to a Ca-enriched silica gel (Ca/Si ≈ 0.5). The calcium hydroxide and carbonate contents were similar in both exposures. After further research using XRD, TGA and ²⁹Si NMR the authors confirmed that the carbonation products formed at 3% CO₂ were representative of the products formed at long term natural carbonation [5]. In agreement, Shah et al. using XRD, TGA and SEM-EDS point analysis found that the products formed at 60% RH, 3% CO₂ compared to products formed at natural carbonation [6]. No results on carbonation at relative humidity higher than 75% were found.

Table 1 presents the summary of pore solution investigations of carbonated cementitious materials found in the literature. For the studies reported in [7, 8], the pore solution was obtained by high pressure squeezing on moisturized samples. Carbonated concrete is usually dry and therefore pore solution squeezed by mechanical procedures requires that the samples are moisturized. The water added in the samples in [7, 8] was however not reported and the dilution was not taken into account when determining the pore solution composition. For the studies reported in [9, 10] cold water extraction (CWE) and inductively coupled plasma mass spectrometry (ICP-MS), a rapid leaching method on ground mortar or concrete, was used to study the pore solution composition.

All studies show that the amount of alkali metals (Na and K) in the carbonated pore solution is reduced compared to pore solution of non-carbonated samples [11]. Anstice et al. [7] found similar amounts of alkali metals in the pore solution of carbonated mortars (first carbonated and then moisturized) at different CO₂ concentrations while higher amounts of sulphates and chlorides were found in the samples exposed to 100% CO₂. Pu et al. [8] reported higher amounts of free alkali metals compared to [7]. The addition of fly ash reduces the amount of alkali metals in the pore solution in non-carbonated samples [11]. The studies reported in [9, 10] using CWE showed that

the amount of free alkali metals in the pore solution of Portland cement and Portland-fly ash cement mortar were similar when carbonated at 60% *RH*, 1% CO_2 , .

The current paper summarizes observations of the impact of different exposure conditions on the microstructure and phase assemblage of carbonated mortar and concrete. Various techniques were applied: SEM-EDS point analysis (chemical composition of the solid phases), optical microscopy (microstructure), cold water extraction (chemical composition of the pore solution), and thermogravimetric analysis (solid phases).

Table 1: Summary of pore solution investigations in carbonated mortar and cement paste found in the literature. T is given in [$^{\circ}\text{C}$], RH in [%] and CO_2 in [%]

Ref	Cement	w/b	Exposure			Technique	Composition				Unit
			T	RH	CO_2		Na	K	Cl	S	
[7]	CEM I	0.6	22		100	Squeezed pore solution (300 MPa) + Ion chromatographic analysis	4	10	21	17	mmol/l
		0.6	22	75 ^a	5		4	9	13	20	
		0.6	22		0.03		3	15	4	1	
		0.6	22		100		2	6	11	15	
		0.6	22	65 ^b	5		7	16	12	24	
		0.6	22		0.03		4	13	8	11	
		0.6	22		100		5	11	23	18	
		0.6	22,	55 ^c	5		0	1	8	2	
		0.6	22		0.03		3	26	8	2	
		0.6	22		100		10	17	23	20	
		0.6	22	55 ^d	5		1	1	11	7	
0.6	22		0.03	1	1	9	5				
[8]	CEM I	0.5	20	40 ^e	0	Squeezed pore solution (300 MPa)	1.1	1020	-	-	mmol/l
		0.5	20	40 ^e	5		0.2	190	-	-	
	CEM II/B-V (15% FA)	0.5	20	40 ^e	0	+ pH meter	0.9	580	-	-	
		0.5	20	40 ^e	5		0.2	190	-	-	
[9]	CEM I	0.55	20	60 ^e	0	CWE + ICP-MS	24	30	1	3	mmol/kg
		0.55	20	60	1		6	2	2	11	
		0.55	20	90 ^f	0		26	30	0	1	
	CEM II/B-V (30% FA)	0.55	20	60 ^e	0		17	23	1	1	
		0.55	20	60	1		5	2	2	12	
		0.55	20	90 ^f	0		17	24	0	0	
0.55	20	90	5	5	3	15	18				
[10]	CEM I	0.55	20	Sealed		26	30	-	-	mmol/kg	
	CEM I	0.55	20	60	1	4	2	-	-		
	CEM II/B-V (30% FA)	0.55	20	Sealed		18	22	-	-		
		0.55	20	60	1	3	1	-	-		
0.40	20	60	1	3	1	-	-				

Note: Salt solutions used to keep RH at a certain value: ^a: sodium chloride, ^b: ammonium nitrate, ^c: magnesium nitrate, ^d: sodium dichromate, ^e: sodium bromide, ^f: barium chloride, CWE: Cold water extraction, ICP-MS: Inductively Coupled Plasma Mass Spectrometry

The aim was to characterize the influence of the exposure condition on the carbonation reaction products. The investigation was part of the larger project with the overall purpose to study the impact of fly ash on the corrosion rate of steel embedded in carbonated concrete. In the corrosion study, exposure to 90% RH, 5% CO₂ was used to promote a relatively high carbonation rate (5% CO₂) and at the same time a relatively high corrosion rate when carbonated [12]. This to limit the need for changing the exposure condition before the corrosion studies. Moisture has a strong impact on the corrosion rate and a well-defined moisture state facilitates the comparison of corrosion rate data in different samples.

2. EXPERIMENTAL

The experimental investigation comprises three sets of series. The investigated materials and exposure conditions (including the used legends) are given in Table 2 and Table 3, respectively. The legends for the samples combine material (fly ash replacement (FA)) and exposure (RH and CO₂), <% FA>-<% RH>-<% CO₂>, e.g. 30-60-1 is a sample containing 30% fly ash which was exposed to 60% RH, 1% CO₂.

Table 2: Material and cement compositions investigated.

Description	Cement type according to EN 197 [13] and fly ash content (FA)		
	CEM I (0% FA)	CEM II/B-M (18% FA)	CEM II/B-V (30% FA)
Series 1 Concrete prisms	x	x	x
Series 2 Mortar prisms			x
Series 3 Mortar disks	x		x

Table 3: Exposure conditions investigated (all 20°C except XC3 (16-22°C)).

Legend	Non-carbonated		Carbonated				
	Sealed cured	Dried at 60%	Non-carb. sample	Natural XC3	60% RH, 1% CO ₂	90% RH, 5% CO ₂	60% RH, 100% CO ₂
	<%FA>- Sealed	<%FA>- 60-0	<%FA>- Bulk	<%FA>- XC3	<%FA>- 60-1	<%FA>- 90-5	<%FA>-60- 100
Series 1			x	x		x	
Series 2	x			x	x		
Series 3	x	x			x	x*	x

* only CEM II/B-V as CEM I samples were not fully carbonated

2.1 Samples

Three commercially available Norwegian cements were used: CEM I (0% FA), CEM II/B-M (18% FA) or CEM II/B-V (30% FA). Tables 4 and 5 provide the chemical composition of the cements.

For Series 1, concrete prism (120*150*260 mm) and wall elements (1200*1500*250 mm) were cast at a concrete plant from concrete ($w/b = 0.55$) containing all three cements. Further information on casting and compaction can be found in [12]. The concrete prisms were kept in the mould for three days and when demoulded wrapped in plastic for 11 days. After this period, the prisms were exposed to accelerated carbonation for 20 weeks. The walls were exposed to natural carbonation in sheltered condition (XC3). Drilled cores with a diameter of 100 mm were investigated.

For Series 2, mortar prisms (140*40*160 mm) containing CEM II/B-V and having $w/b = 0.40$ or 0.55 and paste-to-sand ratio (p/s) of 0.73 in volume were prepared. Further information on casting and compaction can be found in [10]. The mortars were cast in steel moulds and compacted using a vibrating table. Two 20-mm layers were compacted by applying 5 seconds of vibration for the $w/b = 0.55$ and 10 seconds for the $w/b = 0.40$ on each layer. After casting, the prism were covered with plastic for one day and subsequently stored sealed in plastic at 20°C for 13 days. At the age of 14 days, the mortar prisms were exposed for 9 weeks to different conditions.

For Series 3, mortars ($w/b = 0.55$) containing CEM I and CEM II/B-V were mixed and cast in polyethylene bottles 50 mm in diameter and 100 mm in height. Further information in casting and compaction can be found in [9]. Each bottle was filled in three layers and each layer jolt-compacted applying 30 strokes. The bottles were kept sealed at 20°C for two weeks and then wet-cut in disks of 15 mm in thickness using a saw. At the age of 14 days the disks were exposed to different carbonation conditions until they were fully carbonated. When the samples did not show any change in colour after spraying thymolphthalein on a freshly split sample they were classified as “fully carbonated”.

Table 4: Chemical composition and fineness of the cements used in Series 1 by XRF [% by mass].

Cement	% FA	SiO ₂	Al ₂ O ₃	Fe ₂ O ₃	CaO	MgO	SO ₃	P ₂ O ₅	K ₂ O	Na ₂ O	Blaine [m ² /kg]
CEM I	0	19.6	4.9	3.1	60.8	2.3	3.7	0.1	0.9	0.5	548
CEM II/B-M	18	25.5	7.6	4.2	50.7	2.1	3.3	0.2	1.1	0.6	477
CEM II/B-V	30	28.4	8.8	4.4	46.9	2.2	2.7	0.2	1.2	0.6	459

Table 5: Chemical composition and fineness of the cements used in Series 2, 3 by XRF [% by mass].

Cement	% FA	SiO ₂	Al ₂ O ₃	Fe ₂ O ₃	CaO	MgO	SO ₃	P ₂ O ₅	K ₂ O	Na ₂ O	Blaine [m ² /kg]
CEM I	0	20.4	4.8	3.4	61.7	2.2	3.5	0.2	0.9	0.5	420
CEM II/B-V	30	29.5	10.8	4.5	44.6	2	3.2	0.4	1.1	0.5	501

2.2 Methods

Table 6 provides an overview of methods applied and the types of samples used.

Carbonation depth was detected spraying a pH indicator (thymolphthalein, 1%) on a freshly split surface (120*150 mm). For Series 1, carbonation depths were also determined on the thin sections (50*50 mm) using crossed polarized light.

Thin sections were prepared by the Danish Technological Institute according to NT Build 361 [14]. The concrete samples were impregnated with an epoxy resin containing fluorescent dye, mounted on a glass plate, ground to a thickness of 20 μm , and then covered with a glass. The thin sections were investigated with a Leica DM 2500P microscope using polarized, crossed polarized and fluorescent light.

Polished sections containing carbonated, transition zone, and non-carbonated concrete were prepared by the Danish Technological Institute according to [15]. The polished sections were

investigated using scanning electron microscope Quanta 400 ESEM from FEI operated at high vacuum mode, accelerating voltage of 15 kV, spot size 5 and working distance of 10 mm were used. The specimens were carbon coated and the data were Proza corrected. The points were manually selected (typical 50 points in each zone) in the outer hydration products in carbonated and non-carbonated areas avoiding unreacted fly ash, clinker grains and aggregates. During scanning electron microscopy energy dispersive spectroscopy (SEM-EDS) point analysis a volume of approx. $1 \mu\text{m}^3$ comprising a combination of different phases is analysed.

Cold water extraction (CWE) was applied as described in [16] on homogenized ground powder. The powder was passed through 80 μm mesh sieve and mixed with deionized water and filtrated. The filtrated solution was diluted and acidified. The composition of the filtrated solution was analysed using inductively coupled plasma mass spectrometry (ICP-MS). The chemical composition of the pore solution was determined in mmol/kg of mortar.

Thermogravimetric analysis (TGA) was performed on homogenized ground powder using a Mettler Toledo TGA/DSC 3+. Aluminium oxide crucibles were loaded with ca. 300 mg of powder. The samples were heated from 40°C to 900°C at a rate of 10°C/min while the oven was purged with N_2 at 50 ml/min. The weight loss of the samples was monitored as a function of the temperature.

Table 6: Methods applied.

Method		Carbonation depth	Microstructure	Solid phases		Pore solution
		pH indicator	Optical microscopy	SEM-EDS	TGA	CWE
Type of sample		Freshly split surface	Fluorescent thin section	Polished section	Powder	Powder
Series 1	Concrete prisms	x	x	x		
Series 2	Mortar prisms	x				x
Series 3	Mortar disks	x			x	x

3. RESULTS

3.1 Microstructure

Table 7 presents a summary of the characteristics of the microstructure of the paste of the samples investigated in Series 1. Micrographs illustrating the transition from carbonated (top) to non-carbonated (bottom) concrete are given in Figure 1. The micrographs were taken on a CEM II/B-V concrete sample exposed to 90% *RH*, 5% CO_2 using different light settings.

Generally, the concrete samples appear with a plane and intact surface, though several small micro-cracks formed in the plastic stage are present in the surface. The concrete containing CEM II with 18% FA seems to have the highest amount of surface defects.

All the concretes samples have a relatively porous paste as well as a somewhat inhomogeneous paste texture with alternating porous and less porous (patchy) areas. Furthermore, adhesions defects (formed in the plastic stage) between paste and aggregate are observed in most of the concretes. In general, the capillary porosity of the carbonated surface is higher compared to the capillary porosity

of inner non-carbonated paste. However, this higher porosity is not considered an effect of carbonation but an initial defect, formed when the concrete was still plastic.

The paste of the concretes is, dependent on the exposure condition, carbonated to varying depths (Table 7). Deepest carbonation and the most even carbonation front is seen in the concretes exposed to 60% *RH*, 1% CO_2 . The carbonation is also deep in the concretes exposed to 90% *RH*, 5% CO_2 , but the carbonation front is very uneven, varying from 4-15 mm (Figure 1). Lowest depth of carbonation is seen in the natural exposed concrete where the maximum carbonation depth is 5 mm (Table 7).

The carbonation depths determined by the pH indicator and on the thin sections using crossed polarized light are comparable, taking into account the variation of the carbonation front as reported in [17], see Table 7.

Partially hydrated and non-carbonated cement grains are present in the carbonated paste, especially near the surface. This feature is most pronounced in the concretes containing CEM I and CEM II with 18% FA and exposed to natural carbonation or at 60% *RH*, 1% CO_2 . In concrete containing CEM II with 30%FA, and in the concretes exposed to 90% *RH*, 5% CO_2 most of the cement grains in the carbonated paste are fully hydrated and the formed inner C-S-H is fully carbonated.

As the paste in general has a patchy appearance, the carbonated paste also appears patchy with less or even non-carbonated “islands” embedded in carbonated paste. The most distinct patchy feature is seen in concrete without fly ash, and to some extent in the concretes exposed to 90% *RH*, 5% CO_2 .

The concretes containing CEM I and CEM II with 18% FA has a normal carbonation texture, whereas the concrete containing 30% FA a popcorn-like texture is observed.

Other characteristics which were investigated were the presence of CH in the carbonated area or in the bulk, the width of the transition zone from carbonated to non-carbonated concrete, adhesion and surface cracks, and the air content. A characteristic feature of the samples exposed to 90% and 5% CO_2 was a densification in front of the carbonation front. This issue should be investigated in more detail, potentially it is due to an accumulation of sulphates.

Overall, the microstructure of the carbonated concretes depended more on inhomogeneities prior to carbonation (mixing, casting) than on the exposure conditions.

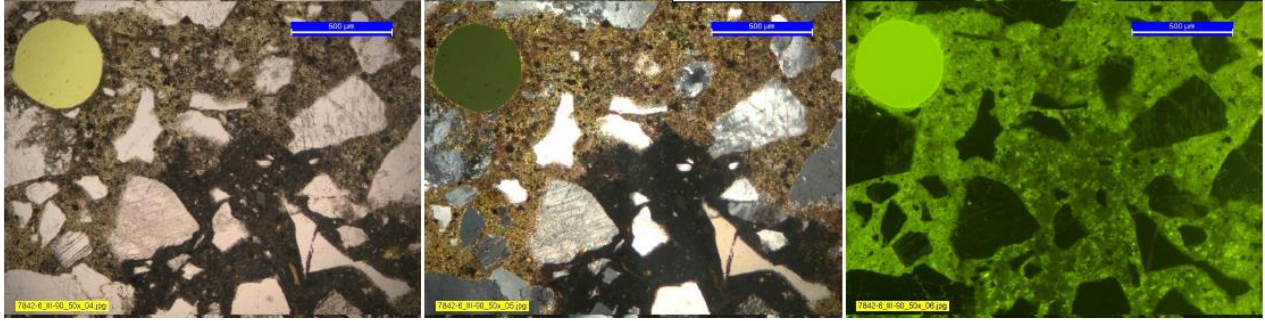


Figure 1: Micrographs illustrating transition from carbonated (top) to non-carbonated (bottom) in 30-90-5 (Series 1). Optical microscopy on fluorescence epoxy impregnated thin sections. From left to right: polarized, crossed polarized and fluorescent light.

Table 7a and 7b: Characteristic microstructure of the carbonated and non-carbonated paste determined on thin sections and carbonation depth determined by thymolphthalein on companion samples (Series 1).

Label	Xc Microscopy [mm]	Xc THY [mm]	Carbonated surface region			Paste porosity, rel. to non-carbonated paste
			Front	Popcorn carb.	Non-carb. islands	
0-60-1	12	12-15	Even	-	Many	Slightly increased
18-60-1	12-14	17-20	Rel. even	-	Some	Slightly increased
30-60-1	20-22	22-25	Rel. even	X	None	Slightly increased
0-90-5	4-14	5-17	Un-even	-	Many	Increased
18-90-5	7-14	8-16	Un-even	-	Few	Increased
30-90-5	11-15	6-20	Un-even	X	Some	Increased
0-XC3	2-5	2.5-3	Un-even	-	Some	Slightly increased
18-XC3	2-5	3.5-5	Un-even	-	None	Slightly increased
30-XC3	4	2.5-4	Even	X	Few	Slightly increased

Note. Xc: carbonation depth (minimum and maximum), THY: thymolphthalein

Table 7b.

Label	Transition zone		Noncarbonated				
	Width [mm]	Porosity	Patchy	Paste porosity	CH	Air, rel. amount	Adhesion cracks
0-60-1	1.2	-	Distinct	High	High	High	Some
18-60-1	1.2	-	Somewhat	Medium	Medium	Low	Many
30-60-1	-	-	Weak	Medium	Low	Low	Some
0-90-5	1	Decreased	Distinct	High	High	High	Few
18-90-5	1	Decreased	Somewhat	Medium	Medium	Low	Few
30-90-5	-	Decreased	Somewhat	Medium	Low	Low	Few
0-XC3	0.8	-	Somewhat	High	High	High	Few
18-XC3	0.8	Decreased	Somewhat	Medium	Medium	Low	Some
30-XC3	1	-	Somewhat	Medium	Low	Low	Some

3.2 Solid phases

Figure 2 presents the differential weight loss curves of the investigated mortar disks (Series 3). Table 8 presents the calculated amounts of CH (calcium hydroxide) and \underline{CC} (calcium carbonate) related to the weight at 850°C. Additionally, Table 8 includes the theoretical maximum amount of \underline{CC} formed upon carbonation assuming all the CaO available in the systems carbonates, and the degree of carbonation related to this maximum amount.

Even for the samples exposed to 100% CO₂, the calculated degree of carbonation was less than 100%. This is probably due to incomplete carbonation of the clinker grains. When comparing the plain Portland cement (0%) samples, a slightly increased amount of carbonates was formed at 100% CO₂ compared to 1% CO₂ (degree of carbonation 70% versus 90%). Compared to 1% CO₂ exposure, the 100% CO₂ exposure led to a reduction of the peak(s) in the temperature range 100-150°C corresponding to calcium silicate hydrate (C-S-H), ettringite (AFt), monosulfate or monocarbonate (AFm) and gypsum. Similar trends are observed for mortar disks with 30% FA. The fly ash samples were also carbonated at 90% RH, 5% CO₂, which led to slightly less carbonates compared to carbonation at 60% RH (degree of carbonation 70% versus 80% and 90%).

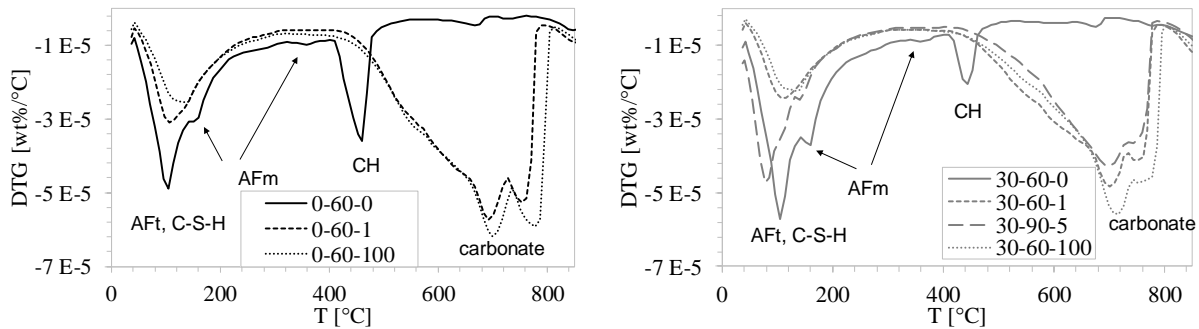


Figure 2: Differential weight loss (DTG) for mortar disks (Series 3) exposed to 60% RH and 0%, 1% or 100% CO₂, and 90% RH, 5% CO₂. Left 0% FA, right 30% FA. After [9].

Table 8: Measured amounts of CH and \underline{CC} [% of weight at 850°C] and calculated theoretical maximum and degree of carbonation (rounded to nearest 5) for mortar disks (Series 3) exposed to 60% RH and 0%, 1% or 100% CO₂, and 90% RH, 5% CO₂.

	CH [%]	\underline{CC} [%]	\underline{CC} [%] Theoretical maximum	Degree of carbonation [%]
0-60-0	4.5	1		0
0-60-1	-	18	25	70
0-60-100	-	22		90
30-60-0	2	1		0
30-60-1	-	15	18	80
30-90-5	-	13		70
30-60-100	-	17		90

The chemical composition of the carbonation reaction products was investigated using SEM-EDS on the polished sections of carbonated and non-carbonated parts of the concrete samples (Series 1). The points were manually selected (typical 50 points in each zone) in the outer hydration products in carbonated and non-carbonated areas avoiding unreacted fly ash, clinker grains and aggregates. This investigation is also reported in [18]. Figure 3 presents a summary of the data. SEM-EDS point analysis data are presented as Si/Ca versus Al/Ca molar ratios in order to identify phases. In a dot plot, a data point lays in between the ideal stoichiometry of the phases it comprises. The ideal composition of the following hydration phases are included: ettringite (AFt), monosulphate (AFm), and portlandite (CH), in addition calcium carbonate (CC) is added. A certain volume is analysed in a SEM-EDS point analysis. This volume will typically contain a mixture of phases and the resulting point lies in between the stoichiometric compositions of these phases. The finer the intermixing of the phases is the fewer points will be near the stoichiometric compositions.

The approximate C-S-H composition of the non-carbonated concretes with fly ash ($\text{Si/Ca}=0.65$) and without fly ash ($\text{Si/Ca}=0.5$) was determined. The Si/Ca decreased to 0.15-0.35 upon carbonation due to the fine intermixing of decalcified C-S-H with CC . The CC originates from the C-S-H, CH and other carbonated hydrate phases. During carbonation, dissolution and precipitation reactions change both the phase assemblage and the distribution of the phases resulting in the fine intermixing of the decalcified C-S-H and CC . Based on the results presented in Figure 3 no clear difference in the composition of the reaction products in the carbonated concretes for the tested cements and exposures conditions could be observed.

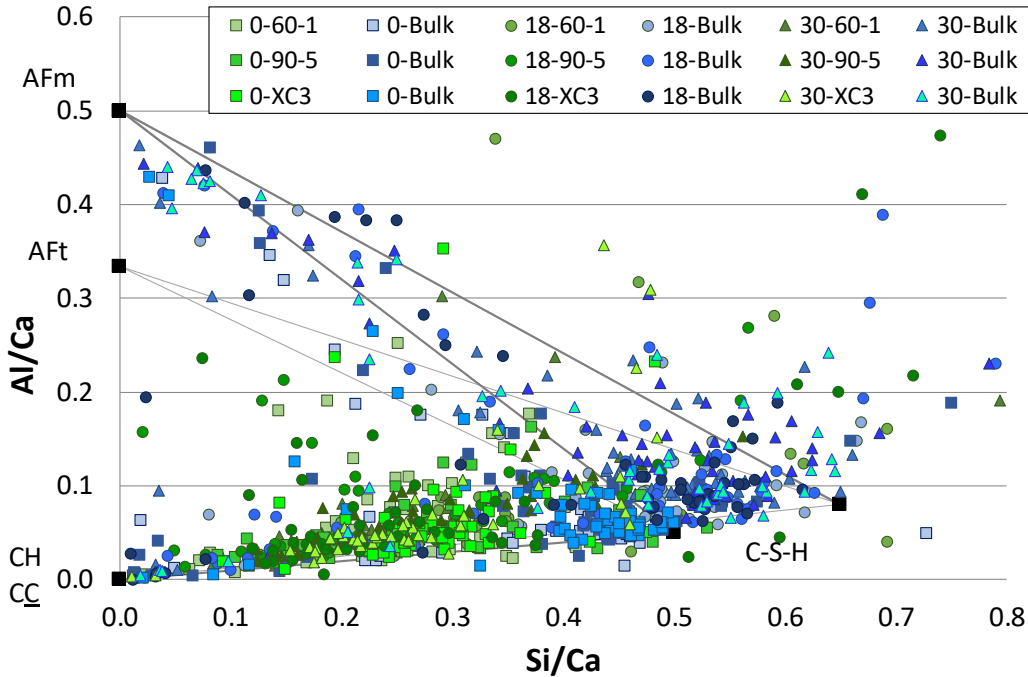


Figure 3: SEM-EDS point analysis data presented as Si/Ca versus Al/Ca molar ratios for carbonated and non-carbonated concrete samples (Series 1). Squares: CEM I (0% FA), circles: CEM II/B-M (18% FA), triangles: CEM II/B-V (30% FA). Green colours: carbonated, blue colours: non-carbonated. After [18].

3.3 Pore solution composition

Data for pore solution analysis of mortar prisms from Series 2 are given in Figure 4. The results include data of the fully carbonated part of the exposed samples (according to the pH indicator) and of the sealed samples. The free alkali metal ion (Na and K) concentrations were lower in the carbonated samples compared to the sealed samples. The sodium and potassium concentrations in the carbonated mortars were not influenced by the w/b (0.40 (30*-60-1) versus 0.55 (30-60-1)). In addition to the data given in Figure 4, the sodium and potassium concentrations of the samples exposed to natural carbonation were measured. These were found to be slightly higher (Na 7, and K 5 mmol/kg) than those of the same samples exposed to 60% RH, 1% CO₂. However, the measured higher free alkali metal contents in the naturally carbonated samples could be due to contamination of the samples with non-carbonated material due to a limited carbonation depth, about 2 mm, after 9 weeks of exposure.

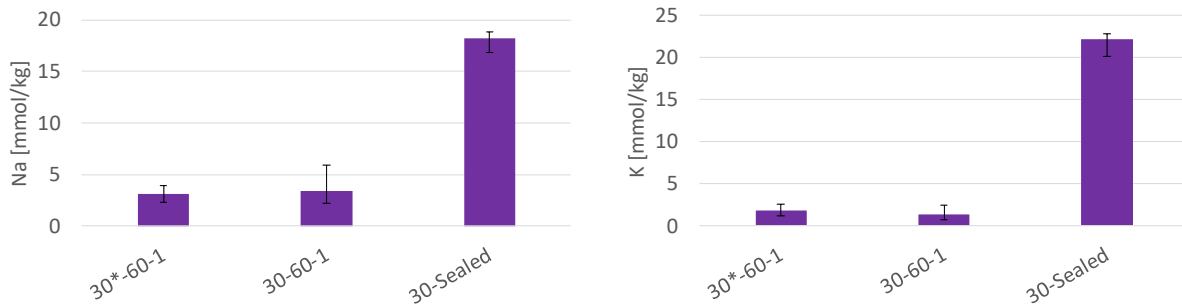


Figure 4: Free alkali metal (Na and K) content (mmol/kg of mortar) using CWE on mortar samples from Series 2. Solid bars (average) and error bars (range) of 3 measurements. Sample 30*-60-1 has $w/b = 0.40$ and 30-60-1 $w/b = 0.55$. Partly after [10].

Figure 5 presents the free alkali metals, sulphur and chloride content of the mortar disks carbonated at different exposure conditions as well as sealed samples as reference (Series 3). The pore solution composition obtained using CWE yielded a comparable sodium and potassium content in the carbonated mortars, irrespective of the cement composition and the exposure. Similar to observations for Series 2 (Figure 4), the free sodium and potassium content was significantly reduced by carbonation. The free sulphur and chloride contents were considerably higher in the carbonated mortars compared to the non-carbonated mortars. The free sulphur content in the carbonated mortars was comparable for the two cements, but slightly higher in the samples exposed to 60% RH, 100% CO₂ than in the samples exposed to 60% RH, 1% CO₂. The free chloride content was slightly lower in the samples exposed to 100% CO₂ than the samples exposed to 1% CO₂. The fly ash samples exposed to 90% RH, 5% CO₂ showed comparable amounts of sulphur and chlorides to the samples carbonated at 60% RH, 100% CO₂.

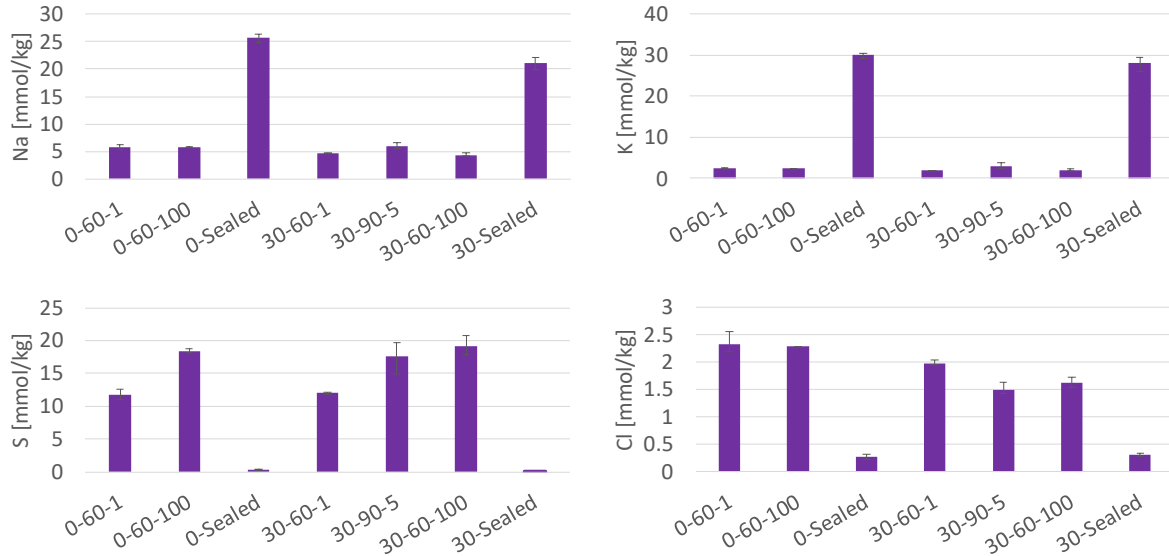


Figure 5: Free alkali metal (Na and K), sulphur (S) and chloride (Cl) content (mmol/kg of mortar) using CWE on mortars from Series 3. Solid bars (average) and error bars (range) of 3 measurements. Partly after [9].

4. DISCUSSION

Petrographic analysis of thin sections revealed that the microstructure of the carbonated samples (natural carbonation (XC3), 60% RH, 1% CO₂, or 90% RH, 5% CO₂) depended more on local initial plastic defects formed prior to carbonation than on the exposure condition or cement type. The concrete containing 30% FA presented a popcorn-like texture in the carbonated zone. As carbonation is a dissolution-precipitation reaction, a difference in the degree of saturation could lead to different distribution. However, with the applied techniques such features were not observed.

TGA indicated that the phase assemblage of samples carbonated at 1% and 100% CO₂ (60% RH, 20°C) is comparable. Difference in moisture content between samples carbonated at 60% and 90% RH does not allow detailed comparison.

SEM-EDS point analysis showed that the composition of the outer reaction products formed upon carbonation were independent of the exposure conditions (XC3, 60% RH, 1% CO₂, or 90% RH, 5% CO₂) and cement types (0-30% fly ash) investigated.

The pore solution analysis of the carbonated samples showed that sodium and potassium are bound by the reaction products upon carbonation, while sulphate and chloride are released into the pore solution. Higher amounts of alkali were found in the naturally carbonated samples compared to samples exposed to 1% CO₂, but it is not clear whether this was due to either the exposure condition or intermixing of carbonated and non-carbonated material during the sampling. The three accelerated carbonation exposure conditions resulted in comparable pore solution compositions.

Table 9 presents a summary of the findings. In summary, the results suggests that accelerated carbonation at 90% *RH*, 5% CO_2 might be used for corrosion studies.

Table 9: Summary of the of findings on the difference in microstructure and phase assemblage due to variation in exposure conditions during carbonation

Exposure	Method	Findings
XC3 60% <i>RH</i> , 1% CO_2	Optical microscopy	<ul style="list-style-type: none"> The microstructure of carbonated samples was similar regardless cement type and exposure condition except that the <u>CC</u> had a popcorn-like texture in the 30% FA samples.
90% <i>RH</i> , 5% CO_2	SEM-EDS	<ul style="list-style-type: none"> The chemical composition of the outer reaction products was similar regardless type and exposure condition.
60% <i>RH</i> , 1% CO_2 60% <i>RH</i> , 100% CO_2	CWE + ICP-MS	<ul style="list-style-type: none"> The amount of free alkali metals (Na and K) upon carbonation was similar regardless the exposure condition and cement type. The amount of sulphates increased slightly upon carbonation at 90% <i>RH</i>, 5% and 60% <i>RH</i>, 100% CO_2 compared to 60% <i>RH</i>, 1% CO_2. The amount of chlorides decreased slightly upon carbonation at 90% <i>RH</i>, 5% and 60% <i>RH</i>, 100% CO_2 compared to 60% <i>RH</i>, 1% CO_2.
90% <i>RH</i> , 5% CO_2	TGA	<ul style="list-style-type: none"> Carbonation at 100% CO_2 slightly increased the amount of carbonates and reduced the phase in the 100-150°C range compared to carbonation at 1% CO_2. At 90% <i>RH</i>, 5% CO_2 slightly less carbonates were formed compared to 60% <i>RH</i>, 1% CO_2.
XC3 60% <i>RH</i> , 1% CO_2	CWE + ICP-MS	<ul style="list-style-type: none"> The results are non-conclusive due to the limited carbonation of the naturally carbonated samples.

5. CONCLUSIONS

The influence of the exposure condition on the carbonation reaction products was studied to assess the applicability of exposure at 90% *RH*, 5% CO_2 of samples for corrosion rate studies of steel embedded in carbonated concrete.

The results suggests that accelerated carbonation at 90% *RH*, 5% CO_2 might be used for corrosion rate studies. The influence of the exposure conditions was minor compared to the changes upon carbonation (from non-carbonated to carbonated state).

ACKNOWLEDGEMENTS

The current investigation is part of a larger research project, ‘Lavkarbsem’ (NFR project no. 235211/O30). The project was supported by the Norwegian Research Council and the following companies: Mapei AS, Norbetong AS, Norcem AS, Skanska AS, and Rambøll Engineering AS. The authors would like to thank Gilles Plusquellec (NTNU at the time the work was carried) and Simon Langedal (NTNU at the time the work was carried) for their experimental investigation which are included in this summary paper. Norcem is acknowledged for XRF analysis of the cements.

REFERENCES

1. Bertolini L, Elsener B, Pedferri P, Redaelli E & Polder R: "Chapter 5: Carbonation-induced corrosion. Corrosion of Steel in Concrete," Weinheim, Germany, Wiley-VCH Verlag GmbH & Co, 2013. pp. 79-91
2. Harrison TA, Jones MR, Newlands MD, Kandasami S & Khanna G: "Experience of using the prTS 12390-12 accelerated carbonation test to assess the relative performance of concrete," Magazine of Concrete Research, No. 64, 2012, pp.737-47
3. Castellote M, Fernandez L, Andrade C & Alonso C: "Chemical changes and phase analysis of OPC pastes carbonated at different CO₂ concentrations," Materials and Structures, No. 42, 2009, pp. 515-25
4. Auroy M, Poyet S, P. LB, Torrenti J-M, Charpentier T & Moskura M: "Representativeness of accelerated carbonation testing of cement pastes," Proceedings, XXII Nordic concrete research symposia, Reykjavik, Iceland, 2014, pp. 447-450
5. Auroy M, Poyet S, Le Bescop P, Torrenti J-M, Charpentier & T, Moskura M: "Comparison between natural and accelerated carbonation (3% CO₂): Impact on mineralogy, microstructure, water retention and cracking," Cement and Concrete Research, No. 109, 2018, pp. 64-80
6. Shah V, Scrivener K, Bhattacharjee B & Bishnoi S: "Changes in microstructure characteristics of cement paste on carbonation," Cement and Concrete Research, No. 109, 2018, pp. 184-97
7. Anstice DJ, Page CL, & Page MM: "The pore solution phase of carbonated cement pastes," Cement and Concrete Research, No 35, 2005, pp. 377-83
8. Pu Q, Jiang L, Xu J, Chu H, Xu Y & Zhang Y: "Evolution of pH and chemical composition of pore solution in carbonated concrete," Construction and Building Materials, No. 28, 2012, pp. 519-524
9. Langedal SL: "Investigation of resistivity, porosity and pore solution composition in carbonated mortar prepared with ordinary Portland cement and Portland-fly ash cement," Master Thesis. Norwegian University of Science and Technology, Trondheim, 2018
10. De Weerd K, Plusquellec G, Belda Revert A, Geiker MR & Lothenbach B: "Effect of carbonation on the pore solution of mortar," Submitted to Cement and Concrete Research, 2018.
11. Vollpracht A, Lothenbach B, Snellings R & Haufe J: "The pore solution of blended cements: a review," Materials and Structures. 2015:1-27, No. 49, 2016, pp 3341–3367
12. Belda Revert A: "Corrosion in carbonated fly ash concrete," PhD Thesis Norwegian University of Science and Technology, Trondheim, 2018
13. EN-197-1. Cement - Part 1: Composition, specifications and conformity criteria for common cements, 2011
14. Nordtest- NT Build 361. Concrete, hardened: Water-cement ratio, 1991
15. Detwiler RJ, Powers LJ, Jakobsen UH, Ahmed WU, Scrivener K & Kjellsen KO: "Preparing Specimens for Microscopy," Concrete International, No. 23, 2001, pp. 50-58
16. Plusquellec G, Geiker MR, Lindgård J, Duchesne J, Fournier B & De Weerd K: "Determination of the pH and the free alkali metal content in the pore solution of concrete: Review and experimental comparison," Cement and Concrete Research, No. 96, 2017, pp. 13-26

17. Belda Revert A, De Weerd K, Hornbostel K & Geiker M: "Carbonation Characterization of Mortar with Portland Cement and Fly Ash, Comparison of Techniques," Nordic Concrete Research, No. 54, 2016, pp. 60-76
18. Belda Revert A, De Weerd K, Geiker MR & Jakobsen UH: "SEM-EDS analysis of products formed under natural and accelerated carbonation of concrete with CEM I, CEM II/B-M and CEM II/B-V," Proceedings, XXIII Symposium on Nordic Concrete Research & Development, Aalborg, Denmark, 2017, pp. 85-88